QUARTERLY TECHNICAL REPORT

15 NOVEMBER 1994 -14 FEBRUARY 1995

OREGON GRADUATE INSTITUTE

DATE OF GRANT: 2/15/93
DATE OF EXPIRATION 8/31/96
GRANT AMOUNT: $2,300,000
GRANT NUMBER: N00014-93-1-0312

DR. C. NEIL BERGLUND, PRINCIPAL INVESTIGATOR
PROFESSOR OF ELECTRICAL ENGINEERING & APPLIED PHYSICS
OREGON GRADUATE INSTITUTE OF SCIENCE & TECHNOLOGY
20000 NW WLAKER ROAD
PO BOX 91000, PORTLAND, OR 97291-1000
TELEPHONE: (503) 690-1591
SOCIAL SECURITY NUMBER: [redacted]
EMAIL: BERGLUND@EEAP.OGI.EDU

DR. A. M. GOODMAN
SCIENTIFIC OFFICER
CODE 1114SS
OFFICE OF THE CHIEF OF NAVAL RESEARCH
800 NORTH QUINCY STREET
ARLINGTON, VIRGINIA 22217-5000
703-696-4218

LOW TEMPERATURE MATERIALS GROWTH AND PROCESSING DEVELOPMENT FOR FLAT PANEL DISPLAY TECHNOLOGY APPLICATIONS

SPONSORED BY
OFFICE OF NAVAL RESEARCH
800 NORTH QUINCY STREET
ARLINGTON, VA 22217-5660

CHARACTERIZATION AND SIMULATION OF THIN FILM TRANSISTORS FOR TRANSIENT THERMAL PROCESSING

V. S. Rao Gudimetla, Assistant Professor

BACKGROUND:

The project goal is to make DC, AC, transient measurements on the TFTs, fabricated by Professor Sigmon and his group at Arizona State University using low temperature processing techniques. From these measurements, SPICE parameters will be extracted and these results will be used for process monitoring and device and process optimization for display applications. This work was started by Rao Gudimetla on 10/1/94 and this technical report is for the period 12/1/94 to 2/14/95. The devices from ASU are expected to be ready during the later part of 1995. Meanwhile, previously obtained measurements on TFTs fabricated at Tektronix Inc. are being used to establish a reliable extraction methodology.

RESULTS:

S-parameter measurements on both the n- and p-channel TFTs of two different gate lengths (12.5 microns and 5 microns) were analyzed, assuming a simple AC equivalent circuit. The emphasis has been to extract the time delay between input and output from the measurements and use that information to extract the mobility of the carriers. The frequency range is from 1 to 200 MHz. The following are the key accomplishments.

1. For the 5 micron devices, the phase of y21 (or S21) was used to estimate the time delay. The experimentally measured time delay was given by:

time delay = (phase of y21 in radians)/(frequency in radians)

The extracted data showed a constant time delay for almost over the entire frequency range of 1 to 20 Mhz both for P and N channel devices. The mobility was estimated using simple equation:

mobility = (Gate length*Gate length)/(time delay* Vds)

The mobility was 100 sq. cm/v-sec for electrons (N channel) and 71 sq. cm/v-sec for holes (P channel). The mobilities remained constant at several Vds values, there by showing that the extraction procedure for mobility is very reliable. For both types of channels, no effects of the gate voltage on mobility were found.

2. For the 12.5 micron devices, the time delay is found to depend on the frequency, suggesting that the capacitance effects are dominant. This may be also due to smaller transconductance values. An effort to adjust the data analysis to account for capacitances has not yet been successful. There is a need to modify the earlier theory of the AC performance of TFTs in the linear region.

3. A graduate student (Loc G. Thai) started working on the device and process simulations of TFTs, that are being fabricated by Professor Sigmon. No measurements were yet done on the Xerox PARC devices due to lack of the lay-out figure.

IMMEDIATE FUTURE PLANS:

1. Modify the AC theory of TFTs to make the extraction of mobility for the long channel devices reliable.

2. We are still collecting the literature on the electrical properties of the grain boundary for use in developing a reliable SPICE model for TFTs. We hope to complete this aspect in the next quarter.

3. Complete the transient measurements on Xerox TFTs.

FIELD EMITTER FLAT PANEL RESULTS

Anthony E. Bell, Associate Professor

Kit-sing Mak, Haibing Liu, Graduate Assistants

Objectives: To develop methods of growing uniform deposits of graphite (fullerene) nanotubes of nanometer scale diameters. It is believed that these field emitters will have the following properties:

1. Low turn-on voltages
2. Insensitivity to the vacuum ambient
3. Inexpensive methods of preparation
4. A compatibility with other industrial efforts - e.g. that of S.I. Diamond Corp.

Method of Approach: Grow nanotubes on Fe nuclei seeded on Si wafers and characterize them by inserting them in a vacuum viewing apparatus with a phosphor screen in order to ascertain the uniformity of electron emission over an area 1 cm x 1 cm. The wafer is heavily doped in order to be electrically conductive and is miscut by 5 degrees so that there will be a uniform density of step edge defects capable of accommodating and attracting the vacuum deposited Fe nanometer scale nuclei on which to anchor the growing carbon nanotubes.

Results: An apparatus to examine the current/voltage characteristics of the nanotube field emitters has been constructed and has a piezo-electric driver so that the cathode and anode separation can be varied. I/V plots as function of separation, d, can be determined.

Work for the next quarter: Various methods of obtaining uniform field emission from the graphite nanotubes will be examined and their electrical and size properties will be investigated.

ELECTROLUMINESCENCE DISPLAY PROGRAM

Rajendra Solanki, Associate Professor

Reinhart Engelmann, Professor

John Ferguson, Graduate Assistant

In order to produce electroluminescent devices which are commercially competitive our effort is being directed towards the creation of full color EL displays. To achieve this it is necessary to find adequate phosphors with the proper brightness and color to work either together as a white light emitting phosphore or separately as three primary color emitters. Our objective during the last quarter was to investigate the light emission from SrS doped with the following rare earth elements: Sm, Tm, Tb, Er, Ho, and Yb.

In order to protect the SrS layer from oxygen and moisture and because of the previously reported success with SrS:Eu grown using the atomic layer epitaxy (ALE) method, the SrS layers for these devices were similarly grown between two ZnS layers. The Sr source consisted of Sr(TMHD), the Zn source was ZnCl, and in both cases the S source was gaseous H_2S. Each of the rare earth elements were doped with a concentration of 10:1 (i.e. one cycle of rare earth atom for every 10 SrS cycles.) In each case the dopant precursor was its respective TMHD complex. Hence, each device grown had the following sequence of thin film layers: ITO, ATO (precoated glass substrate), ZnS, SrS doped with the specific rare earth element, ZnS, and finally Al_2O_3.

The EL emission spectra for each device appear in Figures 1 through 5. These devices were driven at 1000 Hz with a pulse amplitude of 240 V. The characterization results of the SrS are summarized below:

Sm doped SrS:

The emission spectrum (Fig. 1) shows peaks located at 402 nm, 567 nm, 603 nm, and 650 nm. The emission appears orange although some violet is also visible. A maximum brightness of 0.65 fL was achieved for this device.

Er doped SrS:

Fig. 2 shows the emission spectrum for the Er doped device. The peaks are at 410 nm, 527 nm, 536 nm, 553 nm, 558 nm, and 666 nm, with those between 500 and 600 being dominant. This device appears green. A maximum brightness of 2.7 fL was achieved.

Tb doped SrS:

For this sample a large number of peaks are visible in the emission spectrum (Fig. 3): 378 nm, 381 nm, 412 nm, 435 nm, 438 nm, 465 nm, 470 nm, 487 nm, 542 nm, and 582 nm. Here the peak(s) at 542 are dominant. The device emits blue/green light with CIE coordinates of x= 0.25 and y = 0.51. A brightness intensity of 9 fL was recorded for this device.

Ho doped SrS:

Like the Tb device, the Ho doped device also has a number of emission lines as seen in Fig. 4. Peaks are visible at 423 nm, 465 nm, 476 nm, 490 nm, 545 nm, 589 nm, and 660 nm. In this case the peak at 490 appears dominant. The emission of this device appears white/grey. A maximum brightness of 1.95 fL was achieved.

Yb doped SrS:

Finally the emission spectrum of a Yb doped device is shown in Fig 5. In this device a single wide peak exists with the maximum located at 502 nm. This device emits green light with CIE coordinates of x=0.26 and y = 0.54. This device produced a maximum brightness of 9.89 fL.

Tm doped SrS:

Note there is no emission spectrum available for this device. This device emitted very dim grey/white light. Unfortunately, the light was too dim to make any kind of characterization.

As can be seen from these results SrS has considerable promise as a host material in white light emitting EL devices. In addition violet and near UV emission which we believe originates from SrCl (formed at the SrS/ZnS interface) can be seen in the Sm, Er, and Tb doped devices.

A copy of our recent publication on white light emitting EL devices is also attached.

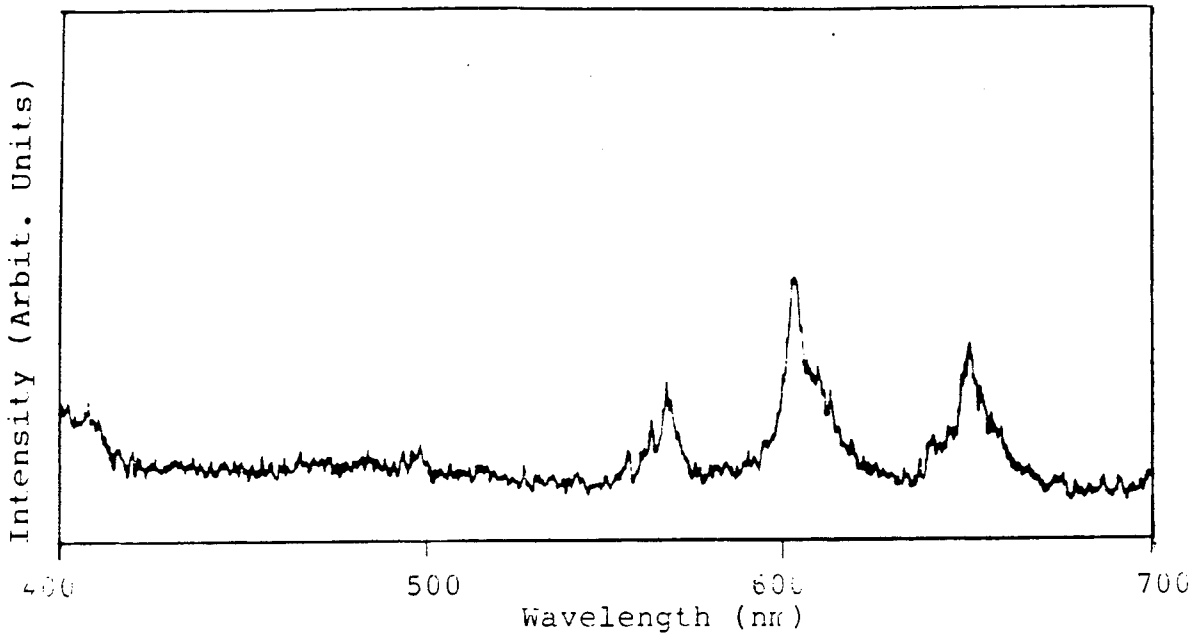

Fig. 1. El emission spectrum for ZnS/SrS:Sm/ZnS device.

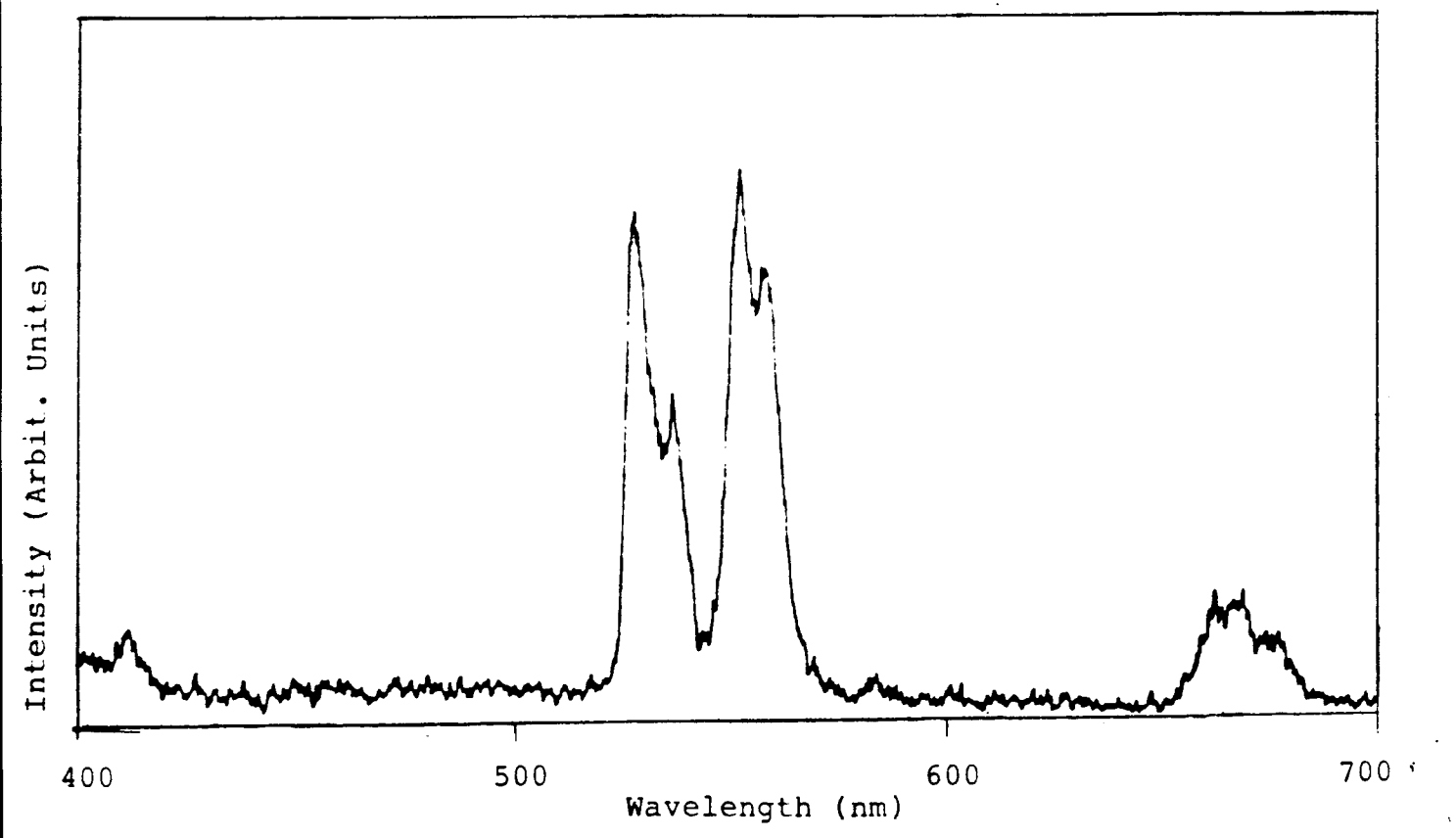

Fig. 2. EL emission spectrum for ZnS/SrS:Er/ZnS device.

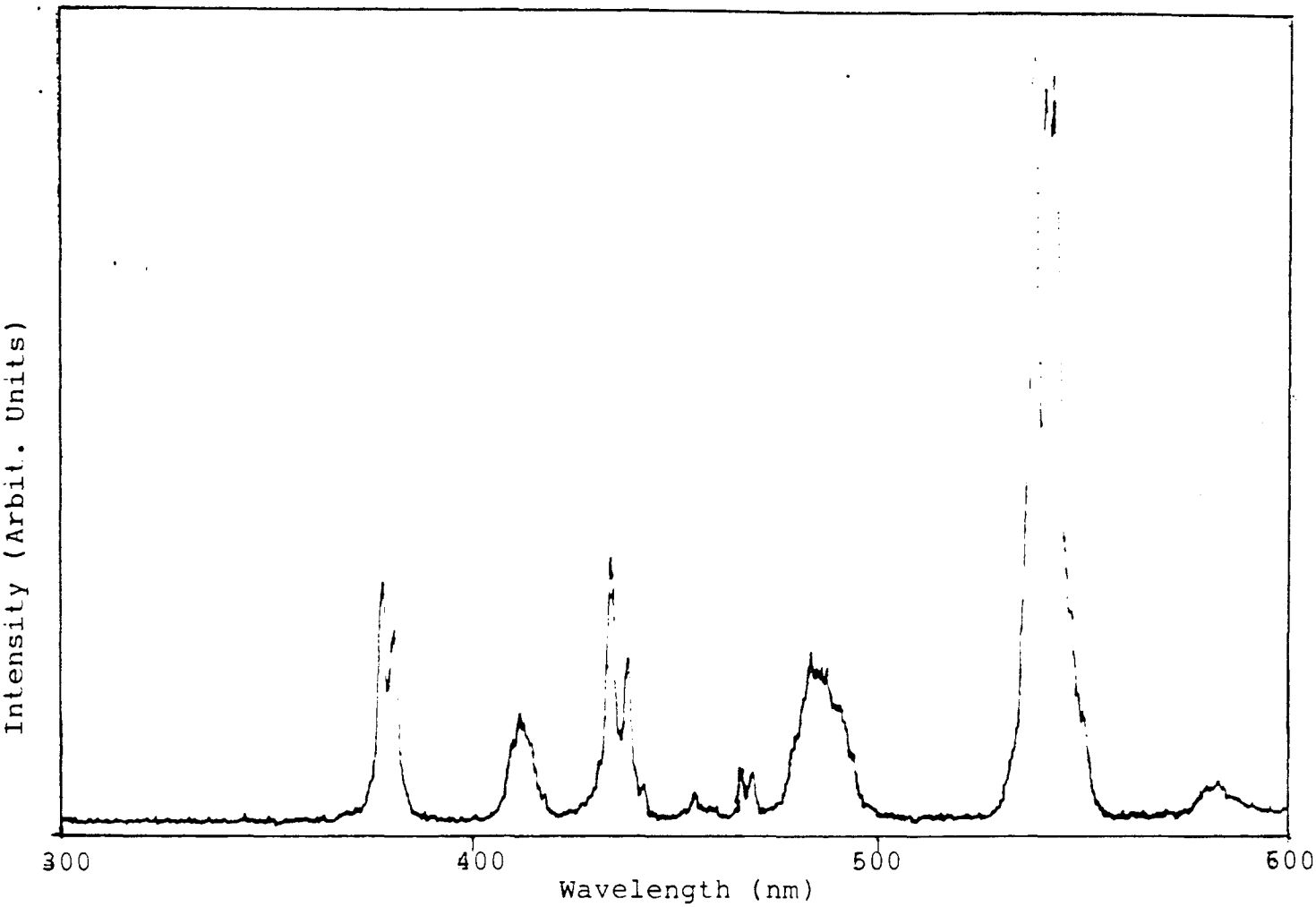

Fig. 3. EL emission spectrum for ZnS/SrS:Tb/ZnS device.

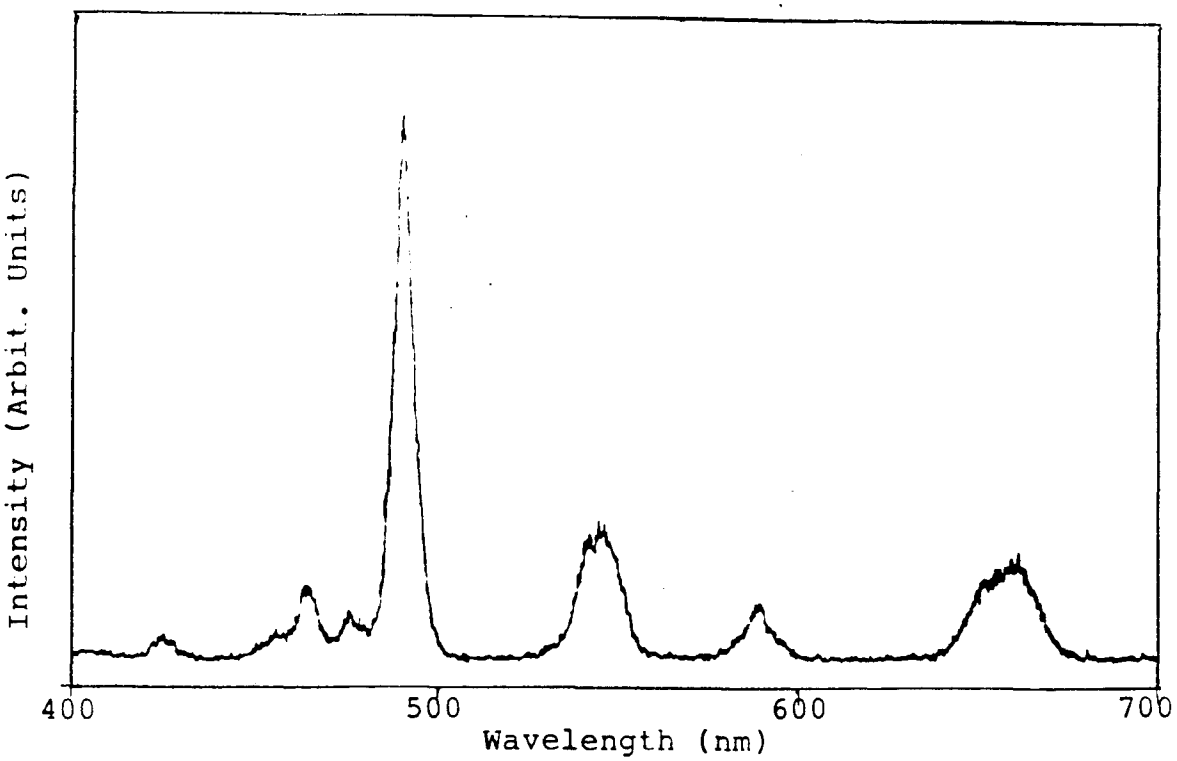

Fig. 4. EL emission spectrum for ZnS/SrS:Ho/ZnS device.

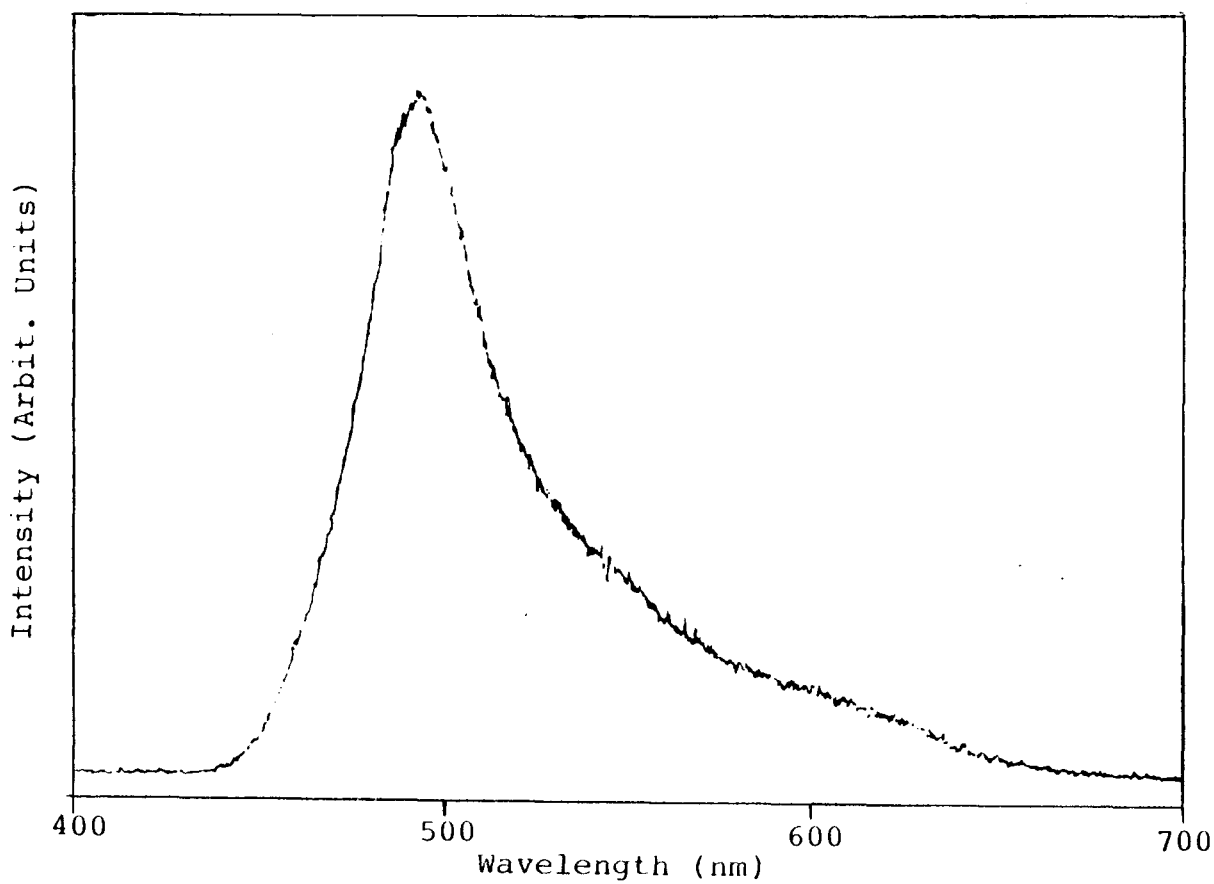

Fig. 5. EL emission spectrum for ZnS/SrS:Yb/ZnS device.

White light emitting SrS:Pr electroluminescent devices fabricated via atomic layer epitaxy

W. Kong, J. Fogarty, and R. Solanki
Department of Electrical Engineering and Applied Physics, Oregon Graduate Institute, P.O. Box 91000, Portland Oregon 97291-1000

R. T. Tuenge
Planar Systems, Inc., Beaverton, Oregon 97006

(Received 9 August 1994; accepted for publication 14 November 1994)

Atomic layer epitaxy has been employed to fabricate white light emitting ZnS:Pr and SrS:Pr thin film electroluminescent devices. Electrical and optical properties of these devices have been characterized and compared. It is found that SrS:Pr devices are significantly brighter and more efficient than ZnS:Pr devices. The effect of ZnS buffer layers on the electrical characteristics of the SrS electroluminescent devices is discussed. © *1995 American Institute of Physics.*

White light emitting electroluminescent (EL) displays are presently of particular interest for producing full color flat panel displays using filters of the three primary colors, as well as egronomically suitable white screens, e.g., for word processing displays. It is believed that the latter application would ease the strain on eyes, for instance for a person looking back and forth at black-on-white text and the screen.[1] To achieve white light emitting displays, several combinations of rare-earth activators have been examined.[2] Among these activators Pr^{3+} luminescent centers are unique in the sense that they produce white light emission by themselves. We describe below the emission of white light from ZnS:Pr and SrS:Pr structures grown using atomic layer epitaxy (ALE).

The Pr^{3+} center in ZnS and SrS hosts has two strong emission bands, one in the red ($^3P_0$–$^3F_2$) and the other in the blue-green ($^3P_0$–$^3H_4$) region. The spectral distribution and the appropriate intensity ratio of the two bands satisfy the complementary color relationship, hence the emission appears white. An advantage of the single over multiactivator doping is that the color generally remains unchanged even if the electrical driving conditions such as the frequency are varied and there would be no energy transfer from one activator to another that could restrict the doping concentrations.[3] On the other hand, Pr^{3+} luminescent center cannot be used as a source for full color displays or backlighting for color liquid crystal displays since its blue-green band is too narrow to obtain sufficient green emission using filters. However, this limitation can be overcome to a certain extent by codoping Pr with Ce, which has a wider blue-green emission band.[4]

The EL devices used for this study had the standard double insulating sandwich structure. The phosphors were grown on glass substrates that had layers of sputtered indium tin oxide (ITO), followed by an aluminum oxide/titanium oxide (ATO) insulator films. The phosphors and the top insulator (Al_2O_3) were grown using a Microchemistry F-120 atomic layer epitaxy reactor. Details of the ALE growth of ZnS and Al_2O_3 have been discussed previously.[5] Two sets of devices were fabricated. One set had 0.26 μm ATO, followed by 0.48 μm ZnS:Pr and finally 0.24 μm Al_2O_3. The second set had the same thickness ATO, followed by 0.1 μm undoped ZnS, 0.46 μm SrS:Pr, another 0.1 μm ZnS layer and a top insulator of 0.24 μm Al_2O_3. The doping concentration of both ZnS and SrS was 1 at. %. The precursor sources for Sr and Pr were their respective beta diketonates (−2,2,6,6-tetramethyl-3,5-heptanedione). One should note that the properties of the commercially available $Sr(tmhd)_2$ are not consistent from one batch to another. For example, the melting temperature, as well as the color of this precursor near the melting point will vary from clear (which produces the best films) to yellow or dark brown. We believe this is due to the impurities in the source.

The purpose of sandwiching the SrS with 0.1 μm ZnS layers is to provide a buffer between SrS and the oxide layers. Due to the high oxygen affinity of SrS, direct contact between it and the oxide insulators would lead to its oxidation. The ALE growth temperature was 400 °C. Aluminum dots (3 mm diameter) were evaporated on the top insulator to serve as the rear electrode. Post deposition grazing incidence x-ray analysis showed that the phases of the polycrystalline SrS and ZnS films were cubic and hexagonal, respectively. The oxide films were amorphous.

These EL devices were typically powered by bipolar pulses of 30 μs duration with 5 μs rise and fall times and a frequency of 1 kHz, unless otherwise noted. The EL emission spectra of ZnS:Pr and SrS:Pr devices are shown in Fig. 1. In both cases, the emission consists of one strong band in the blue-green region and another in the red. These bands in the SrS:Pr spectrum show several sharp peaks which are believed to be due to crystal field splitting of the $^3H_4$ and $^3F_2$ energy levels. The lack of fine structure in ZnS:Pr has been attributed to lattice distortion introduced by the large radius Pr^{3+} ion (radius 1.01 Å) on the Zn^{2+} (radius 0.74 Å) site.[6] In the case of SrS, Sr^{2+} ion (1.13 Å) has a comparable radius to Pr^{3+}. However, the phase difference of the host lattices was not taken into consideration and the wide bands due to $^3P_0$–$^3H_5$ and $^3P_0$–$^3H_6$ transitions in both ZnS and SrS cannot be explained at this time. It is interesting to note that at liquid nitrogen temperature, the band due to $^3P_0$–$^3H_5$ transition gets significantly attenuated in both ZnS and SrS spectra. Apparently this transition is induced due to some form of phonon coupling.

 0003-6951/95/66(4)/419/3/$6.00

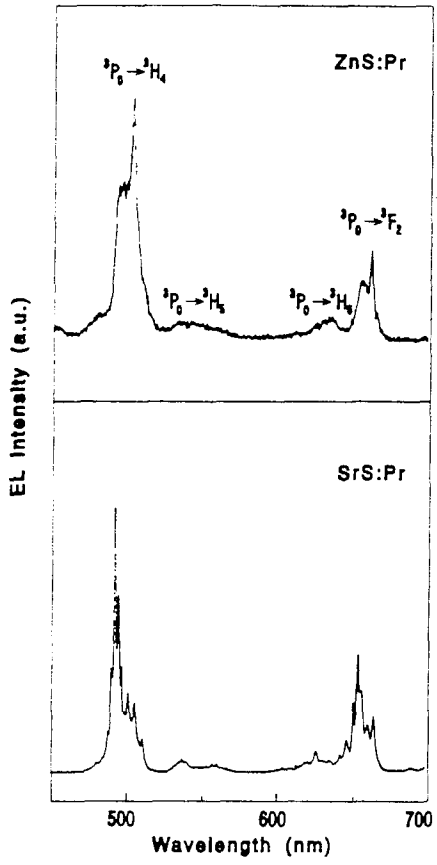

FIG. 1. Emission profiles of ZnS:Pr and SrS:Pr electroluminescent devices.

The emission lifetimes of ZnS:Pr were about a half of SrS, as shown in Table I. The light emission efficiency of ZnS:Pr is also about an order of magnitude less than SrS:Pr. This difference could be due to one of several reasons. As mentioned above, stress due to the large Pr ion distorts the ZnS lattice. Also, the Pr ion has different environments in the two different crystalline phases. It has been also proposed that the $(4f)(5d)$ excited state of Pr^{3+} lies close to the conduction-band minimum of SrS. Therefore, the EL excitation process is aided by the energy transfer following host excitation, in contrast to ZnS:Pr where the dominant excitation mechanism is believed to be direct impact excitation by the hot electrons. These differences could account for the large difference in their luminescent efficiencies listed in Table I. The appearance of both the devices was white as evident from the CIE (Commission Internationale de l'Eclairage) coordinates (Table I). Typical brightness of the two types of devices (at 40 V above the threshold) is also presented in the table. It is interesting to note that the brightness of SrS:Pr and ZnS:Pr devices increased at liquid nitrogen temperature by factors of 3 and 20, respectively, indicating strong phonon coupling in the latter. The enhancement in brightness in both types of devices was consistent with an increase in the measured transferred charge at low temperature as discussed before.[5] The brightness and efficiency of the ALE grown ZnS:Pr and SrS:Pr EL devices are about the same as those grown by sputtering and electron beam evaporation.[3,6] However, we cannot make direct comparison to those devices[3,6] since there is no information about the phase of their phosphor materials and unlike our devices, their phosphors were codoped.

TABLE I. Comparison of the optical characteristics of ZnS and SrS EL devices.

Property	ZnS:Pr	SrS:Pr
Lifetime (μs)	17	33
CIE coordinates		
X	0.31	0.36
Y	0.39	0.39
Efficiency (lm/W)	0.01	0.2
Brightness (fL)		
at 3.0 kHz, 40 V above threshold	1.5	30

The SrS devices have a strong affinity for oxygen and water vapor. Therefore, as mentioned earlier, ZnS layers are used to buffer this phosphor. However, this creates another set of interfaces, besides the pair between ZnS and the oxide insulators. As a result, the electrical characteristics of these devices display an interesting $I-V$ behavior. Unlike most devices where the conduction current is turned on at a single threshold voltage and then saturates, in this case there are two current thresholds, i.e., with increasing voltage, the conduction current has two sharp turn ons. A drop, followed by an increase in conduction current with increasing field has been reported in other devices and explained as originating either from long lifetime bulk traps or multilevel energy levels of the electron trap sites at the phosphor/insulator interface.[7] However, in our device, based on $I-V$ and light emission profiles we do not believe either of these to be the case.

The SrS device consists of three semiconductor layers (ZnS/SrS/ZnS). We propose that the two thresholds are due to two different breakdown voltages of ZnS and SrS. Comparing the electrical and light emission profiles of several ZnS and SrS test structures, it was evident that in our devices, SrS had a lower breakdown voltage than ZnS. When the SrS in the SrS/ZnS device breaks down, the conduction current flows across this layer as shown in Fig. 2. After the SrS layer breaks down, as the electric field within the SrS layer is being clamped, the polarization charge continues to build up at the SrS/ZnS interface. This charge further enhances the field in the ZnS layers. The carriers extracted from the SrS/ZnS interface collisionally excite the Pr activator and produce the first hump of light emission profile shown in Fig. 2. As the external field continually increases, the ZnS layers eventually breakdown. When this occurs, the emitted light shows a second peak, however the amount of additional light produced is not large. To see what is happening, consider the current and the light signals in Fig. 2. We know from our previous work that the light pulse closely follows the profile of the current pulse. As the voltage is increased, first the SrS breaks down and the current increases and saturates as in a normal EL device. The light pulse also increases, reaches a peak, and starts to decay. As the voltage is further increased, ZnS breaks down and there is more current now flowing in the device. At this point there is a small increase (~10%) in amount of light emitted although an in-

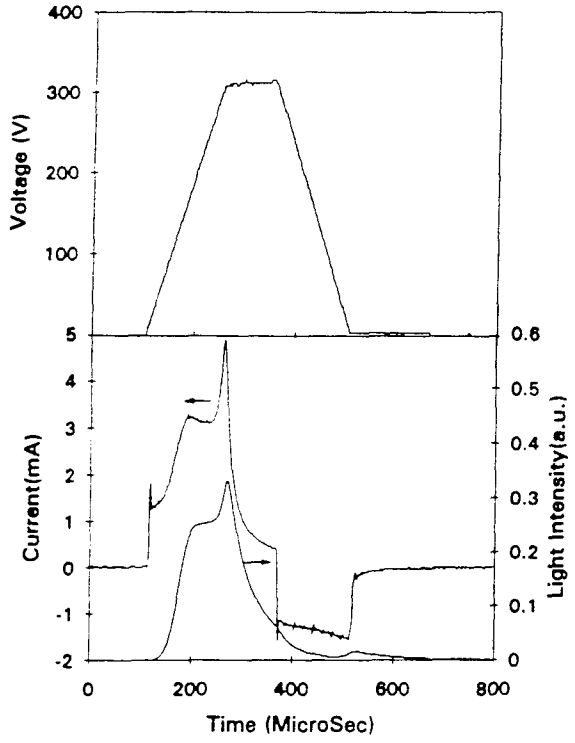

FIG. 2. Applied voltage pulse across the SrS:Pr EL device and its corresponding current and optical emission response.

crease in conduction current in the device of almost 100% is observed. We expect the number of activators diffused into the undoped ZnS to be very small, moreover ZnS excitation efficiency is less, as mentioned earlier, therefore the second peak of light should originate in the doped SrS layer. It appears that the carriers originating at the ZnS/oxide interface are responsible for this second peak of light. Although a large current traverses through the ZnS layer, most of the carriers are most likely trapped at the SrS/ZnS interface. A fraction of these carriers tunnel out into the SrS which then excite the Pr activator. If the total current produced at ZnS/oxide interface were to transverse the entire SrS/ZnS phosphor thickness, then the second peak would have been significantly stronger. The double voltage breakdown was checked using Stimulated Program with Integrated Circuit Emphases (SPICE) simulation, where an equivalent circuit similar to Davidson *et al.*[8] was utilized. In our case three pairs of back-to-back Zener diodes were considered to simulate ZnS/SrS/ZnS structure. This simulation showed good agreement with the current profile shown in Fig. 2. At the end of the voltage pulse, a small light signal is observed which we believe is due to recombination in the SrS layer. The reverse current responsible for this light pulse can be observed at higher magnification.

In summary, we have fabricated while light emitting electroluminescent devices using atomic layer epitaxy. In comparing SrS and ZnS devices, the former are brighter and more efficient. Our next objective is to optimize the active layer thicknesses and doping concentrations to increase the brightness of these devices.

This work is supported by ARPA under Contract No. N00014-93-1-0312

[1] Y. A. Ono, M. Fuyama, K. Onisawa, K. Tamura, and M. Ando, J. Appl. Phys. **66**, 5564 (1989).
[2] R. Mach, in *Solid State Luminescence*, edited by A. H. Kitai (Chapman & Hall, New York, 1993), p. 229.
[3] S. Tanaka, H. Yoshiyama, J. Nishiuva, and S. Ohshio, SID 88 Digest (1988), p. 293.
[4] Y. Abe, K. Onisawa, K. Tamura, T. Nakayama, M. Hanazono, and Y. A. Ono, Jpn. J. Appl. Phys. **28**, 1373 (1989).
[5] W. Kong, J. Fogarty, and R. Solanki, Appl. Phys. Lett. **65**, 670 (1994).
[6] S. Tanaka, S. Ohshio, J. Nishiura, H. Kawakami, H. Yoshiyama, and H. Kobayashi, Appl. Phys. Lett. **52**, 2102 (1988).
[7] V. Singh and S. Krishna, J. Appl. Phys. **70**, 1811 (1991).
[8] J. D. Davidson, J. F. Wager, R. I. Khormaei, C. N. King, and R. Williams, IEEE Trans. Electron Devices **ED-39**, 1122 (1992).